Journal of Mechanical Engineering Research and Developments
ISSN: 1024-1752
CODEN: JERDFO
Vol. 43, No. 4, pp. 165-179
Published Year 2020

Towards High Mechanical Properties and Wear Resistance for Cutting Tool made from Alumina/MWCNTs Composite

Sameer Hashim Ameen[†*], Randa Kamel Hussain[‡], Rasool R. K. Al-Arkawazi[†]

[†]Technical Instructors Training Institute, Middle Technical University, Iraq

[‡]College of Science, Physics Dept., Mustansiriyah University, Iraq

*Corresponding Author Email:dr.sameer.hashim@mtu.edu.iq

ABSTRACT: The ordinary cutting tools used in the traditional turning machines have low wear resistance during the cutting process, especially in their tips, and therefore low or medium life of tools results in a high cost in replacing and consumptions of time. The present work provides a new and good suggestion with a high quality of the tooltip material made from a composite material consisting of alumina as a matrix and different amounts by weight of MWCNTs with 0.5 %, 1.0%, 1.5 %, 2.0 %, and 2.5 % as filler. The experimental investigations were carried out in the current work to study and assess the performance of new material of different compositions in comparison with ordinary tools. The experimental part included several stages; from preparing the nanocomposite powder, sampling, characterization (the structural and morphology properties by XRD and SEM), and compression test to investigate the mechanical properties of all new composites. The XRD manifested the principal peak of the plane (440) due to alumina and the peaks of planes (101) and (110) belong to MWCNT. The XRD confirmed the nanostructure of the composite. Moreover, FESEM evidenced the regular texture morphology that elucidated the localized filler over the matrix. The compression test provided lower modulus of elasticity values with a higher addition of nanocarbon, and then a higher wear resistance is gained. The numerical part was investigated by simulation of a cutting tool using ANSYS PROGRAM v.11 which based on the finite element method. The numerical results depend mainly on the mechanical properties of the experimental part. A significant reduction in the wear reached to 9.24%, 20.75%, 39.2%, and 71.50% for 1%, 1.5%, 2.0%, and 2.5% after the addition of nanocarbon, respectively for 1 mm cutting tool feeding, as a result of maximizing the elastic deformation in the expense of lowering plastic (wear) deformation.

KEYWORDS: Alumina; MWCNT; Nanocomposite; Cutting tool; ANSYS; Wear resistance

INTRODUCTION

Machining is a universal technique of removing chips from a workpiece by using tool having a hard and strong tip [1]. The single-point cutting tool (SPCT) generates symmetrical surfaces from the turning cylindrical shapes. The symmetrical surfaces are determined by removing unwanted material to reach finally the desired shape and size of a workpiece in lathes which is rotating about a fixed axis [2]. Not only the lathe machines but also the other machining processes, like boring, planning, and shaping use SPCT as a cutting tool in borer, planers, and shaper machines, respectively [3]. The cutting process is developed by three perpendicular forces (F_x, F_y, and F_z), wherefore the study and analysis of these forces in addition to cutting parameters (speed, feed, and depth of cut) are represented the core of cutting process [4]. Ceramics composites are favorite in cutting tool due to ceramics properties such as heat shock resistance, chemical stability, and wear resistance [5]. High performance of ceramics composite was obtained by material properties designing to enhance heat resistance keeping the influential hardness. Many materials assumed as an insert material, classically carbides are the most common material used in the cutting tool, it reaches up to 45 % in the year 2000 contrasting with high-speed steel which is used less than 35 %, as shown in Figure 1. New materials entranced to this application with rapidly usage grown to 8 % for cermet (TiC or TiN or both with nickel as binders), 5 % for ceramics, and 4 % for PCD, while 3 % for other materials from the year 2000 to 2018[6]. Many ceramics composites were prepared to improve physical and mechanical properties, such as Al_2O_3/SiC [7, 8], mixed ceramic of Al_2O_3/TiCN that coated to decrease the friction of cutting tool [9]. The sintering of Al_2O_3/ZrO_2 composite at 1400^o C a accompanies with soaking increased the density and hardness that effective on the cutting tool performance [10]. The MWCNTs improved the mechanical properties of the cutting tool to a wide range when

added to composite or as coating material with excellent performance in tribology with lower friction between the contact surfaces and higher resistance to wear [11]. The density and mechanical properties of nanocomposite alumina / MWCNTs depends directly on the weight percentage of MWCNTs due to their excellent wear and friction characteristics [12]. The only low amount of MWCNTs (at least 5 %) could lower both coefficient of friction and penetration of cutting tool depth [13].

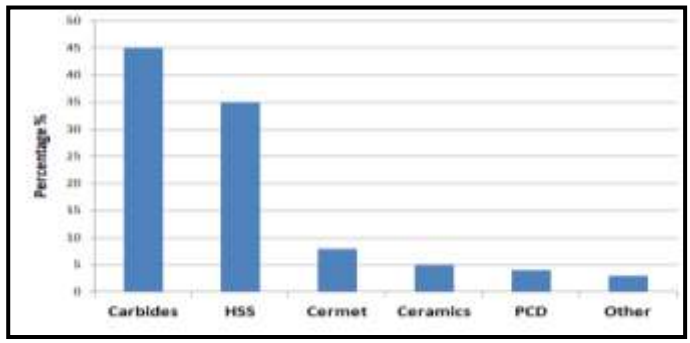

Figure 1. Cutting tools percentage usage.

A weight ratio 0.5 % of MWCNTs in SiC/MWCNTs nanocomposite enhanced both bending strength and hardness compared to the sintered silicon carbide, which increases in fracture toughness to approximately 10 % [14]. The increase in fracture toughness reached to 32 % when only 0.1 % by weight of MWCNTs was used in Al_2O_3/MWCNTs [15], also the scratch resistance and fracture toughness are improved when adding (0.5 % by volume) of graphene to alumina in addition to minimizing the brittleness [16].

This work aims to synthesis a nanocomposite of Al_2O_3/MWCNTs as an insert part (edge of cutting tool) to the main cutting tool body (HSS) to produce a tooltip that has high mechanical properties and superior wear resistance, and then study their properties. Numerical simulation and analysis of thermal, stresses and deformations are performed in order to examined and assessed the optimum composition of the cutting tool.

METHODOLOGY

The main process that carried out in the present work can be seen in a block diagram as follow:

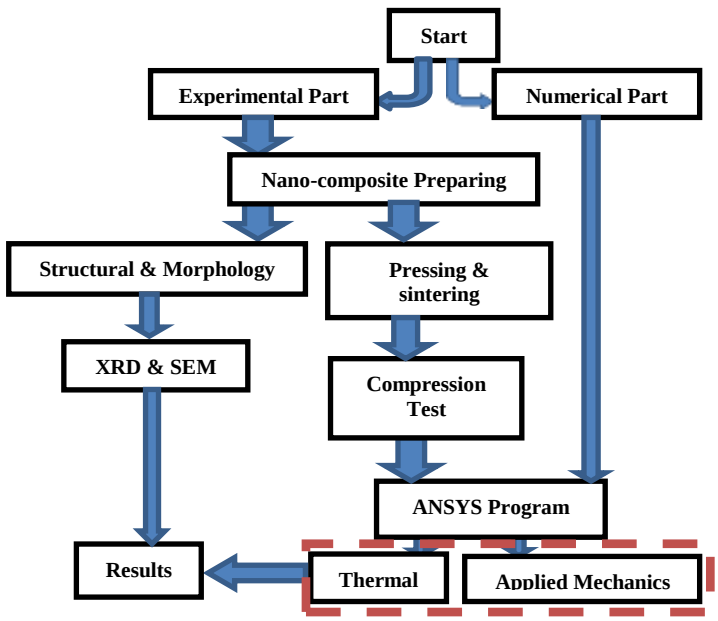

THEORY

The cutting forces that are applied from the cutting tool to the workpiece in the three dimensional axes can be listed as follows [17]:

$$P_y = C_p \times t^x \times S^y \times K \quad (1)$$

$$P_x = 0.3\ P_y \quad (2)$$

$$P_z = 0.2\ P_y \quad (3)$$

Where,

$$K = K_c \times K_\varnothing \times K_\sigma \times K_m$$

In the present work, the five depths of cut (0.2, 0.5, 1.0, 2.0, and 2.5 mm) are considered, and by substitution into equations (1), (2), and (3), the three components of cutting forces are determined, as listed in Table 1.

Table 1. The applied cutting forces for different cutting depths [17].

Cutting forces (N)	S (mm)				
	0.2	0.5	1.0	2.0	2.5
P_x	4.94	12.34	24.68	49.36	61.70
P_y	16.45	41.13	82.28	164.55	205
P_z	3.29	8.23	16.45	32.91	41.13

The power is developed due to the axial movement of cutting tool through a mild steel workpiece of 10 cm diameter and 300 rpm spindle mean speed in the y-direction, it can be estimated from the formula:

$$\text{Power} = P_y \times V_y \quad (4)$$

Where, $V_y = \omega \times R = \frac{2\pi NR}{60}$

The heat generated from the frictional contact of the cutting tool face and workpiece shown in Figure 2 is determined as follow:

$$Q = \frac{Power}{A} \quad (5)$$

The heat flux is subjected to contact area (43 mm^2), which is taken in the present work, and the initial surface temperature for the thermal investigation can be summarized in Table 2 for 300 rpm spindle speed.

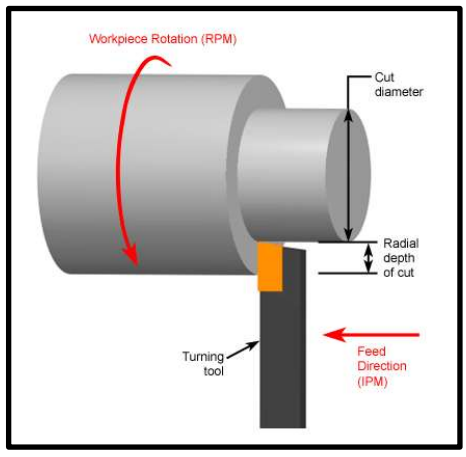

Figure 2. Mechanism of cutting process

Table 2. Heat flux and surface temperature for different cutting depths [17].

Item	S (mm)				
	0.2	0.5	1.0	2.0	2.5

Q (W/m^2)	1408	3520	7043	14083	17552
T (°C)	120	160	200	450	550

During wear process in the workpiece, the relationship connected the moduli of elasticity with hardness is as follows [18]:

$$h_e = h - h_p = \frac{H*\pi*a}{E_r} \quad (6)$$

$$\text{Where, } \frac{1}{E_r} = \frac{1-\vartheta_i^2}{E_i} + \frac{1-\vartheta^2}{E} \quad (7)$$

$$\text{Hence, it can be said the wear resistance} = K\frac{H}{E_i} \quad (8)$$

Where, k is a constant.

The dimensions of h, h_e, and hp are clearly shown in Figure 3. The principal idea is investigated in current work depends on the fact that total penetration of cutting tool (h) is constant, so any further increase in the elastic depth (he) produces a good minimizing of plastic depth (hp); therefore less amount of wear is gained finally.

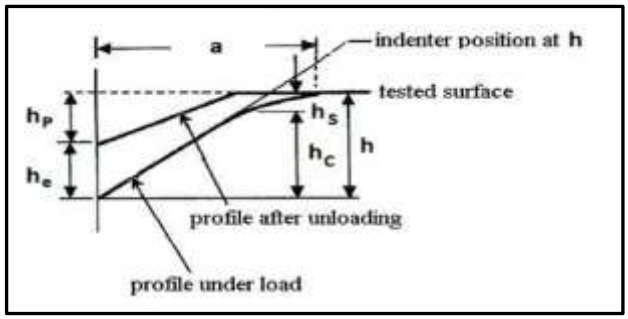

Figure 3. Schematic of wear region in the workpiece [18]

CASE STUDY

The dimensions of cutting tools, which are made mainly from high speed-steel and a cutting tip of alumina – MWCNTs nano composite, are shown in Figure 4.

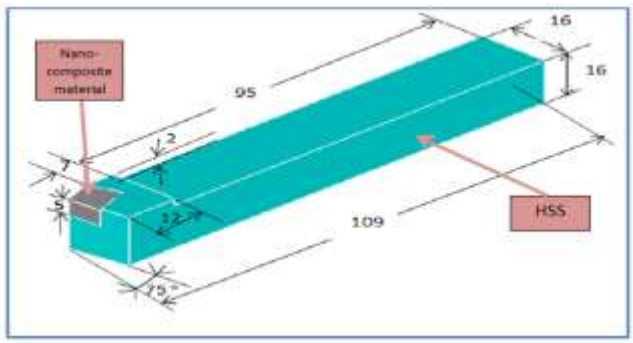

Figure 4. Layout of the current cutting tool

MATERIALS AND PREPARATION

Started materials are commercially available are used without any further purification processes. The synthesis of prepared procedure for Al_2O_3/MWCNT composite is based on the dispersion of the started materials and mixing them into a colloidal solution without any additional complicated chemical treatments. Carbon nanotubes were dispersed into 100 mL ethanol with the aid of ultrasonic agitation for 2 hours. The ultrasonic vibration combined with heating to 60°C was sufficient to distribute the aggregation of MWCNT. The color of

the suspension solution converted completely from transparent to black referring to diffuse the agglomerate MWCNT. The aluminum oxides were collided in 200 mL ethanol and mechanically stirred for 1 hour. The mixture of the two suspensions was collided together keeping the continuous stirring and exposing to the vibration of the ultrasonic agitation waves to ensure the occurrence of the homogenous mixing. Filtering and then washing via distilled water were repeated many times to remove the residual ethanol. Finally, drying in the air and then in the oven at 70°C was done for 2 hours. The resultant powder composites with 0.5%, 1%, 1.5%, 2%, and 2.5% weight ratio of Al_2O_3/MWCNT were formed to the cylindrical shape using the punch – die rig as shown in Figure 5-a. The final form of the sample size was obtained after applying 8-ton weight (730 MPA), which has a diameter of 11.7 mm and a height of 21 mm, as shown in Figure 5-b. The sintering process was carried out for all samples in a digital controlled furnace at temperature 1450°C, as shown in Figure 6. Firstly, the gradual increase in temperature was to 500°C and staying at this degree for 30 minute time interval. Then, the furnace temperature was further increased to 1000°C and kept at this degree for about one hour. Finally, further increasing to the sintering temperature of samples (1450°C) was done before maintaining at this degree for about 2 hours.

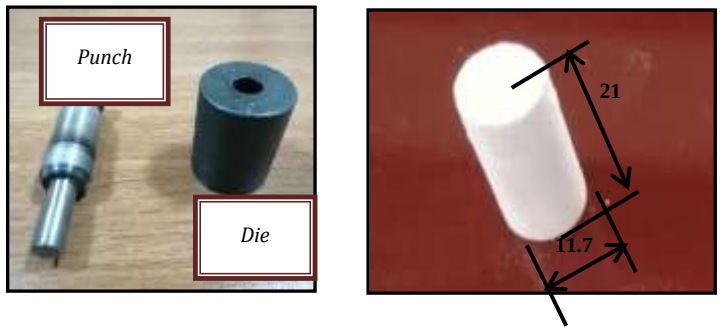

Figure 5. Hydraulic press rig (a) Punch and die, and (b) Final sample shape in (mm) after pressing

Figure 6. The furnace.

RESULTS AND DISCUSSIONS

Structural and Morphology

The physical structural and morphology properties were investigated by x-ray diffraction (XRD) and field emission scanning electron microscope (FESEM) analysis. X-ray diffraction was recorded by (Cu/Kα-1) source radiation with wavelength (1.54059 nm) in angle range 10-80°. Figure 7 displays the XRD pattern of the selected Al_2O_3/MWCNT composite comparing with the raw alumina ceramic. According to the JCPDS card no. (41-1487), the principal peaks positioned at $2\theta=67^0$ correspond to the reflection of plane (440) due to alumina, also many secondary peaks appeared belong to the reflections of planes (012), (022), (104), (400), (422) and (620). The two main peaks lied at $2\theta=42^0$ and 71^0 are corresponding to the reflections from (101) and (110) planes confirming the presence of MWCNT. The intensity reflections of peaks (101) and (110) planes increased as the MWCNTs content. It seems that the Al_2O_3 embedded with nanotubes of carbon. The crystallite size (D), the micro strain (ε) and dislocations density (δ) are calculated using Deby-Sherrer Equations (9) and (10) [19]:

$$D=\frac{K\lambda}{\beta \cos\theta} \quad (9)$$

Where, K is constant (0.89), **λ** is the wavelength of x-ray (1.54056 A), and β is the full width at half maximum of a peak.

$$\varepsilon = \beta \cos(\theta/4) \quad \text{and} \quad \delta=1/D^2 \quad (10)$$

Table 3 lists the filler effects on the crystal size, micro strain and dislocations density that are estimated by XRD. Alumina is a fragile ceramic, a feature causing splinter of micro crystals to nano crystal induced from the ultrasonic waves during the preparation processing.

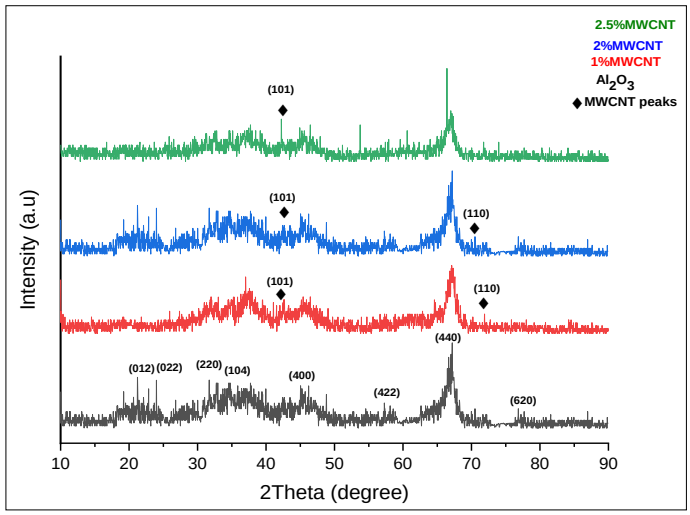

Figure 7. The XRD analysis of pristine Al_2O_3 and selected Al_2O_3/MWCNT

Table 3. The average values of crystal size and micro strain

MWCNTs wt. ratio	D (nm)	ε	δ (nm^{-2})
1%	3.72	$8.2 X10^{-3}$	0.048
2%	5.28	$6.5X10^{-3}$	0.035
2.5%	7.92	$4.3 X10^{-3}$	0.015

The microstructure of pristine alumina and alumina/MWCNT composite photographed at a high magnification of FESEM is displayed in Figures 8 and 9. The FESEM images evidenced that the microstructure of the composite totally differs from that of the pure ceramic of alumina. The comparison of Figure 8-a with Figure 9 indicated that the grains of the ceramic matrix embedded with the MWCNT, which is expected to be a significant effect on the mechanical properties due to interface between the composite phases.

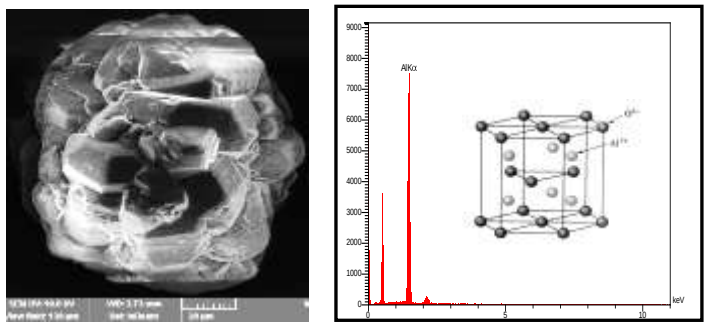

(a) (b)

Figure 8. Pure alumina: (a) FESEM micrographics of structure and (b) EDX analysis

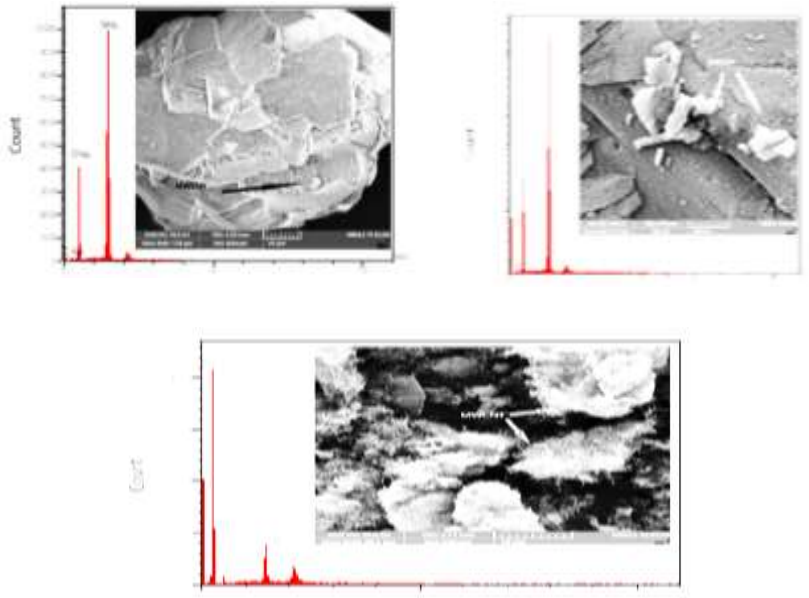

Figure 9. FESEM and EDX analyzing of (a) 1%, (b) 2%, and (c) 2.5% of Al_2O_3/MWCNT

It appears that the ceramic Al_2O_3 ordered in a monolith structure, and it is looked having smaller grains compared to the grains in composites. This could be attributed to the ratio of grain diameter to MWCNTs diameter difference in the raw alumina comparing to composites. The localized MWCNTs possess an average diameter of 10 nm around the alumina matrix grains not inner the matrix giving rise the average grain diameter that is in conformity with ref. [13]. This may agree with results indicating to the reduction in the micro strain, Table 3. At higher additive content, the MWCNTs covered the ceramic grain and the MWCNTs located around the ceramic grains, not within grains. This nano filler localized around the matrix will offer the mechanical properties, significantly affected by the interfacial properties between matrix and filler. For Figure 10, the morphology of nanocomposites 2 wt% MWCNT ensures the homogeneous distribution MWCNTs in the alumina matrix. The carbon nanotube gives raise a soft textile. The elemental compositions and their concentrations were measured by EDX analyzer, the spectrum peaks shown are due to the K electron shell of α-line for Al element, as revealed in Figures 8 and 9. Al element peaks are higher than other; carbon peaks are high at the higher MWCNTs sample content. All peaks kept in their positions without the occurrence of shifting, and no other peaks of foreign elements were appeared.

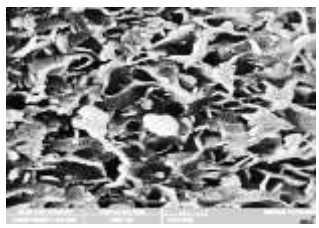

Figure 10. The photographic FESEM of the nanocomposites 2 wt % MWCNT surfaces

The alumina has a high density as a result of the absence of pores and mass transport by diffusion, while the MWCNTs additives provide a higher porosity to the composite [20]. Sintering will reduce the density of alumina; led to a higher amount of MWCNT in a composite. The existence of MWCNTs in the grain interfaces as concentrations masses works as dissolution immobility preposition the grains boundaries, as that the MWCNTs acts an origin of obstruction of grain growing during high temperature treatment [21-22]. The concentrations masses at more ratio adding of MWCNTs could lowered the grain boundaries adhesion attributed to the MWCNTs existence, thus increasing the porosity [23].

Compression Test

The mechanical properties of different composites of alumina as matrix material and the percentage addition by weight of MWCNTs of 0.5%, 1%, 1.5%, 2%, and 2.5% as filler were determined. The compression rig is

shown in Figure11 which consists of stationary and moving discs. The constant speed of the upper moving disc is maintained at 0.5 mm/min until fracture.

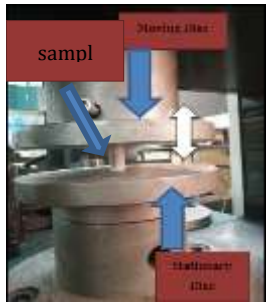

Figure 11. Compression rig.

The stress–strain curves for the selected alumina, alumina with 1% wt. and 2% wt. of MWCNTs are illustrated in Figure 12. The alumina stress–strain response presents the ultimate stress without a clear yield point, while after adding the nanocarbon to alumina, the yield points can be detected, which means that the new composite material performance is like metals (especially steel) with a good convergence of the all mechanical properties of Al_2O_3/2.5% wt. MWCNTs to steel. The MWCNTs, as filler material, occupied all the spaces between the alumina grains which worked to reduce the elasticity of composite material as mentioned before, except 0.5% wt. filler, improved the mechanical properties to 2.25%, 15.15%, and 3.38% for the modulus of elasticity, yield stress, and ultimate compression stress, respectively, as illustrated in a Table 4. The comparison of the alumina results with the ref. [24], giving a good convergence despite the different conditions of production between the two cases. The second comparison was made between the moduli of elasticity of the present work with the ref. [4] as shown in Figure 13, indicating a good convergence in the performance of the two curves with different nanocarbon additions.

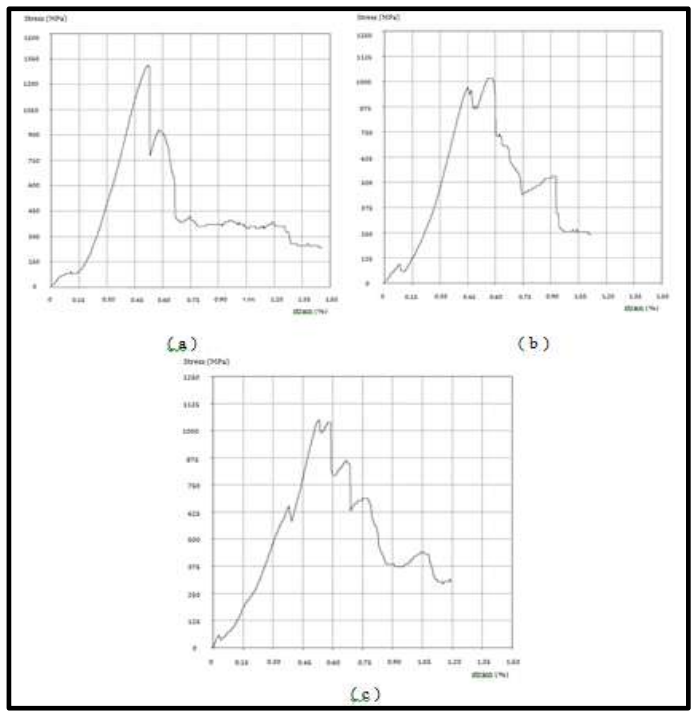

Figure 12. Stress-Strain diagrams: (a) Pure alumina, (b) 1% wt. MWCNTs, (c) 2 % wt. MWCNTs

Table 4. The mechanical properties of alumina and its composites.

material	E_i (GPa)	σ_y (MPa)	σ_u (MPa)
Alumina [24]	---	752	1038

Alumina (present)	355	845	1300
0.5% wt. MWCNTs	363	973	1344
1.0% wt. MWCNTs	325	975	1025
1.5% wt. MWCNTs	294	673	1036
2.0 % wt. MWCNTs	255	650	1050
2.5 % wt. MWCNTs	207	550	753

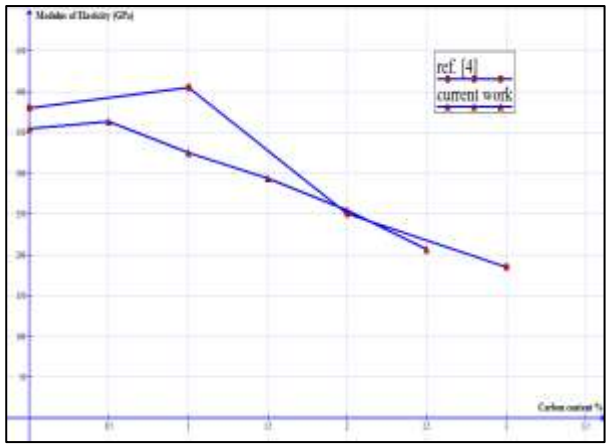

Figure 13. Modulus of elasticities versus the percentage of carbon content.

The Equations (6), (7) and (8) proved that the lower modulus of elasticity and high hardness provide a higher elastic dimension (h_e) and thus a higher resistance to wear. In the current work, a lower modulus of elasticity was obtained by the further addition of nanocarbon by weight to alumina. A higher hardness achieved in the tool tip due to the dispersion of nanocarbon in the spaces between the grains which resulted a stiff surface against the cut.

Numerical Results

In the present investigation, the ANSYS v.11 program was taken as a numerical simulation technique of cutting process. The mesh of cutting tools consisted of 594 elements and 1178 nodes, while the tooltip (nanocomposite materials) refined its nodes, as depicted in Figure 14. The application of the three forces is compensated by a single resultant force, which is converted later to constant pressure on the friction area (5 mm x 8.6 mm) as shown with the boundary conditions of a cutting tool in Figure 15. It is supposed that the density and Poisson's ratio are $\rho = 3690$ kg/m^3 and $\nu_i = 0.22$ for the all composite-materials.

The maximum deformations developed in the cutting tools are 0.02891, 0.01642, and 0.01794 µm for HSS, pure alumina, and alumina with 1% wt. carbon, respectively as shown in Figure 16, indicates that using alumina in the tooltip reduced the deformation to a large amount in comparison with HSS about 176%. It is observed that the addition of 1% wt. of MWCNTs minimized the deformation to 161%.

The maximum von-Misses stress developed in the cutting tool, due to applying 2.033 MPa pressure results from friction between tooltip and workpiece, is 11.953 MPa for HSS, while this value changed slightly to 11.897 MPa for pure alumina and 1% wt. of MWCNTs, as manifested in Figure 17. The factor of safety are 61, 71, and 82 after dividing the yield stresses 724, 845, and 975 MPa by the maximum von-Misses stress for HSS, alumina, and alumina with 1% wt. of MWCNTs, respectively, where the adding 1% wt. of MWCNTs to alumina leads to the increased in the factor of safety of composite to 15.5%. These values of safety factor are sharply increased for cutting depth (feeding) more than 1mm.

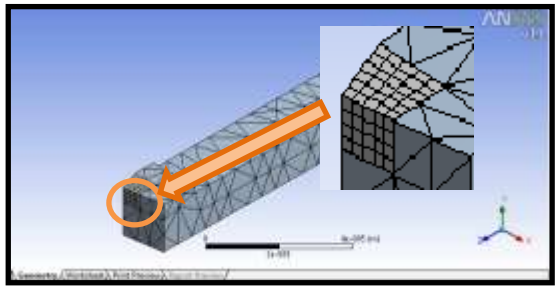

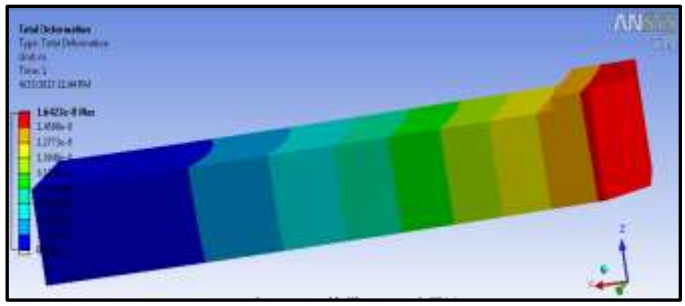

Figure 14. Meshing of cutting tool

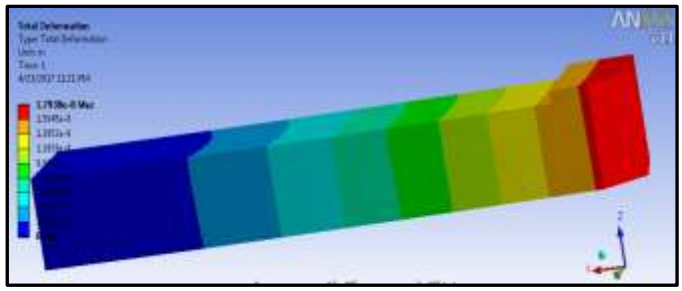

Figure 15. Boundary conditions and loading of 1.0 mm feed for the applied mechanics solution

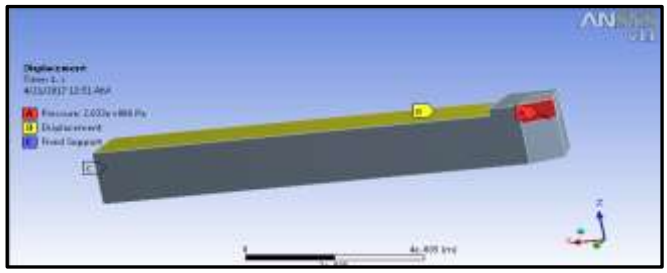

(a)

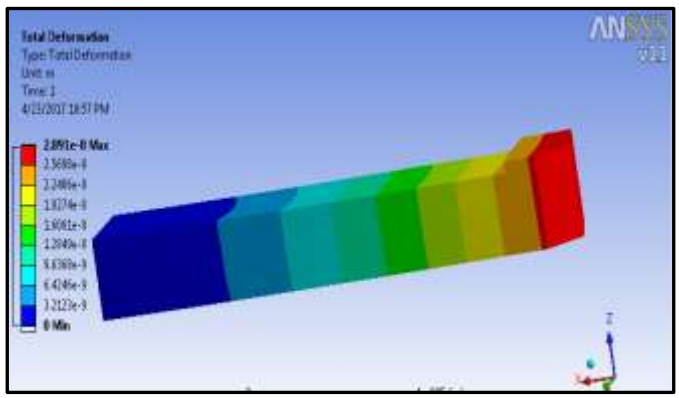

(b)

Figure 16. Maximum deformation (in m) in the cutting tool for 1 mm feed (a) HSS, (b) Pure alumina, and (c) Alumina with 1% wt. MWCNTs

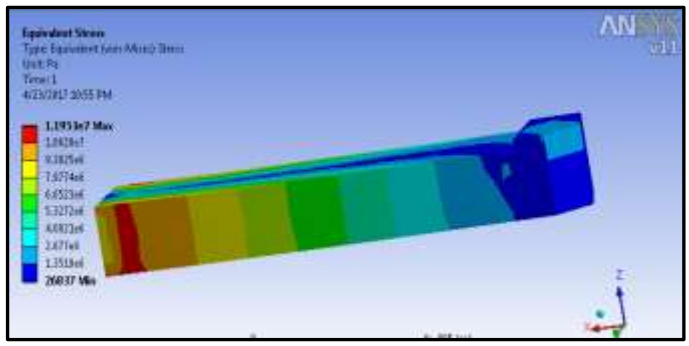

(a)

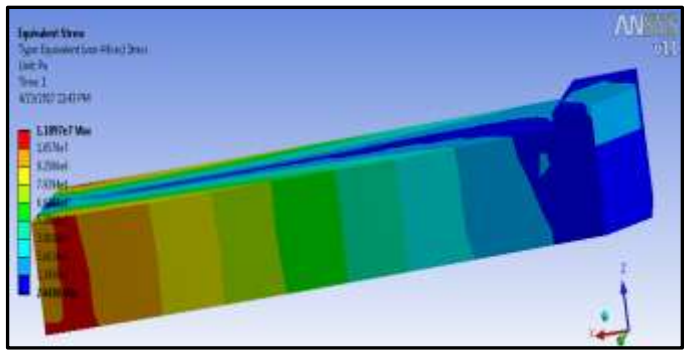

(b)

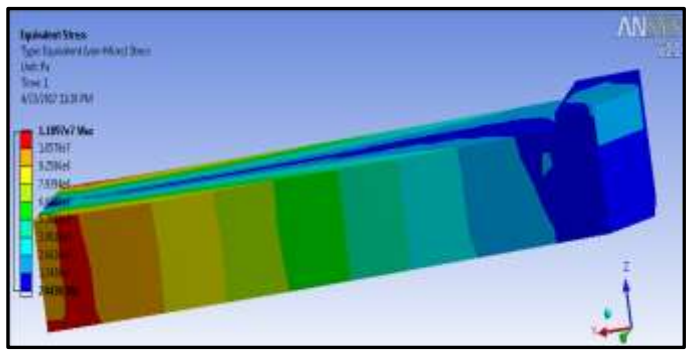

(c)

Figure 17. Maximum von-Misses stress (in N/m^2) in the cutting tool (a) HSS, (b) Pure alumina, and (c) Alumina with 1% wt. MWCNTs

The effect of MWCNTs content on the maximum deformation is elucidated in Figure 18 for different feed penetration of cutting tools in a workpiece. The curves demonstrated an increasing in the elastic deformation (h_e) as increasing MWCNT content, meaning that according to the Equation (6) and Figure 2, a super minimizing in (h_p) is obtained, which is determined from ($h_p = h - h_e$). Hence, a good reduction in wear reached to 9.24%, 20.75%, 39.2%, and 71.50% for 1%wt., 1.5%wt., 2.0%wt., and 2.5%wt. MWCNT, respectively for 1 mm cutting tool feeding. The general behavior that appeared in Figure 18 showed progress in deformation with MWCNT content at specific feeding value. Also, the deformation is increased when feeding rising for fixed Wight ratio MWCNT content.

The von-Misses and shear stresses are increasing linearly versus feeding of a cut as shown in Figure19 for 1% weight of MWCNTs adding to alumina. The increase in the feeding of cutting tool is demonstrated by higher compression stress due to friction.

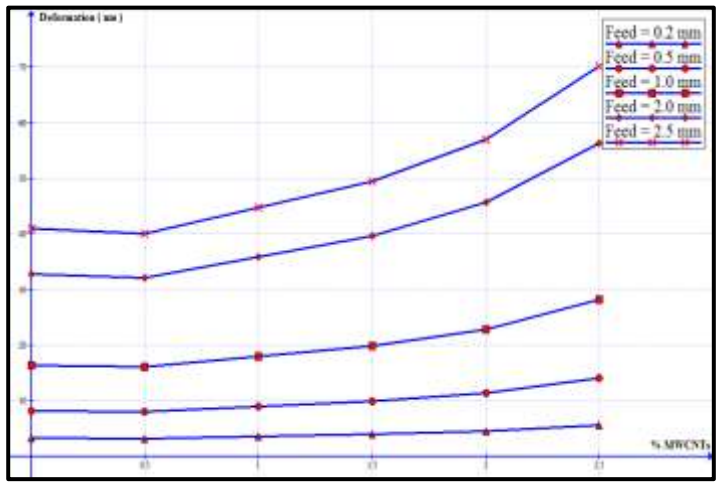

Figure 18. Maximum elastic deformation (in nm) versus the percentage of nanocarbon addition

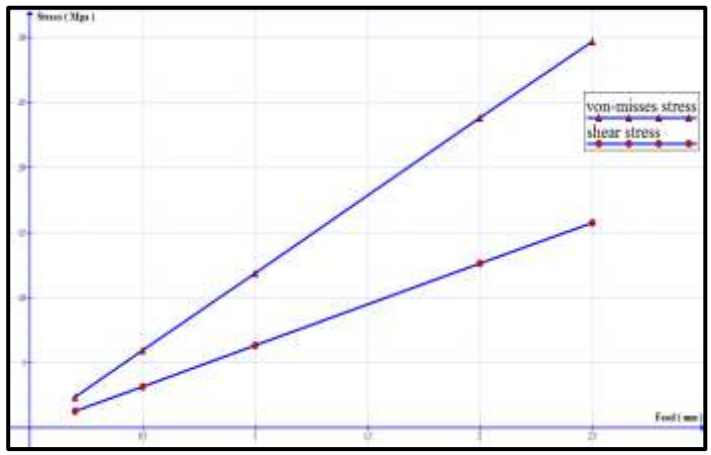

Figure 19. Stress versus in (MPa) versus the cutting feed

For a thermal investigation, the boundary conditions for temperatures and the applied heat flux for 1.0 mm feed are presented in Figure 20, while the gradient of heat flux and the temperature distribution on the cutting tool are displayed in Figures 21 and 22, respectively which are identical for all Al_2O_3/MWCNTs compositions. The increment in the maximum temperature and heat flux values due to more cutting feeding are showing in Figure 23. The excessive friction between the adjacent surfaces of the cutting tool and workpiece occurs during the further feed of cut is generated which causing increase both temperature and heat flux.

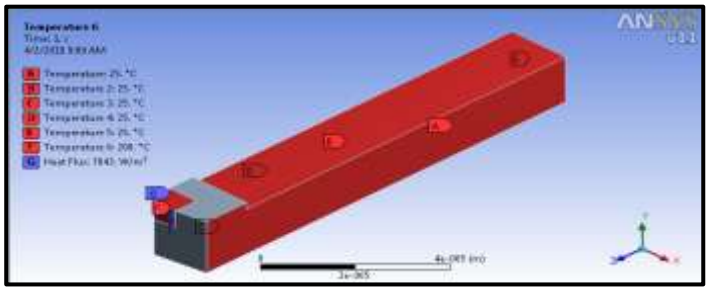

Figure 20. Boundary conditions and loading of 1.0 mm feed for heat solution

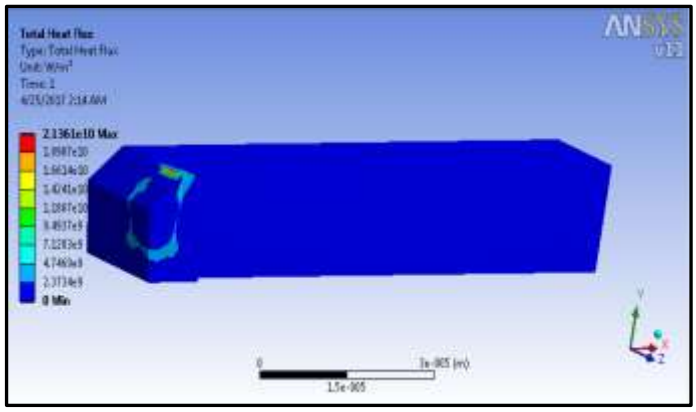

Figure 21. Total heat flux (in W/m^2) for the cutting tool

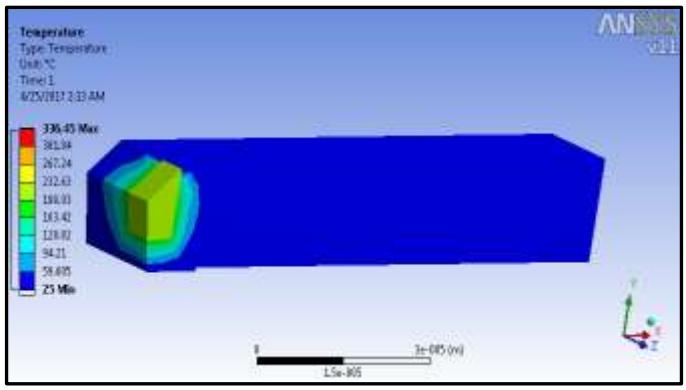

Figure 22. Temperature distribution (in ^oC) for the cutting tool

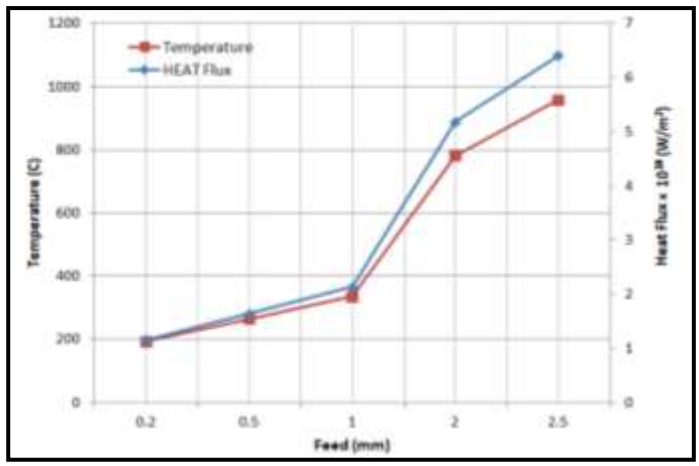

Figure 23. Thermal items versus cutting feed

CONCLUSION

1) The prepared nanocomposites Al_2O_3/MWCNTs exhibited a uniform distribution in the microstructure with an average crystal size in the range of 3.72-7.92 nm, which benefits the uniform distribution of the load that prevents dislocation and then the wear.

2) The MWCNTs localized around (not inner) the alumina grains, the MWCNTs acts as immobility of the grains boundaries that enhanced the mechanical properties of the composite surface and prevent the propagation of crack later.

3) The value of wear is reduced to 9.24%, 20.75%, 39.2%, and 71.50% for 1%, 1.5%, 2.0%, and 2.5% after the addition of MWCNTs to Al_2O_3 respectively for 1 mm cutting tool feeding, due to minimizing the plastic deformation (wear) in the expense of an increasing in the elastic deformation.

4) A significant reduction in the moduli of elasticity for the all composite materials understudy is obtained, where all composites of Al_2O_3/MWCNTs have higher mechanical properties than an ordinary cutting tool made from HSS.

5) The von-Misses and shear stresses are increasing linearly versus the feeding of a cut for the selected composition of Al_2O_3/MWCNTs with a higher factor of safety than an ordinary cutting tool made from Al_2O_3 only and HSS reached to 15.5 % and 34.4 % respectively, and the improvment in mechanical properties is obtained by the suggested material.

6) Similar values of maximum temperatures and heat fluxes of all composites of Al_2O_3/MWCNTs are obtained, for specified feeding of cut, in comparison to a cutting tool made only from Al_2O_3o or HSS which avoiding more heat generation, therefore no excessive thermal stresses developed from suggested materials. Linear increasing in mentioned thermal items with more feeding is noticed.

7) Increasing the content of nanocarbon in alumina serves to change the stress-strain curve response from polymers to the metals, which next demonstrate the yield point clearly. This study proves that the low content of MWCNTs as filler to Al_2O_3 makes mechanical properties similar to steel structures behavior.

REFERENCES

[1] S. Rathod, M. Razik, "Finite Element Analysis of Single Point Cutting Tool," *International Journal of Modern Engineering Research (IJMER)*. http://www.ijmer.com/papers/Vol4_Issue, vol. 3, 2014.

[2] J.P. Davim, Machining of hard materials: *Springer Science & Business Media*, 2011.

[3] M.N. Patil, "Shreepad Sarange Finite Element Analysis of Von Misses Stresses and Deformation at Tip of Cutting Tool," *IJIRAE*, vol. 1, pp. 211-217, 2014.

[4] R. Patidar, S. Sharma, "Effect of Rake Angles on Tool during Orthogonal Metal Cutting Process for Different Materials through Ansys", *International Journal of Engineering Trends and Technology (IJETH)*, Vol. 44, No. 2 pp. 141-145, 2017.

[5] A. Vereschaka, A. Batako, A. Krapostin, N. Sitnikov, G. Oganyan, "Improvement in reliability of ceramic cutting tool using a damping system and nano-structured multi-layered composite coatings," *Procedia CIRP*, vol. 63, pp. 563-568, 2017.

[6] G.T. Smith, Machine tool metrology: An industrial handbook: *Springer*, 2016.

[7] D. Hong, Z. Yin, S. Yan, W. Xu, "Fine grained Al2O3/SiC composite ceramic tool material prepared by two-step microwave sintering," *Ceramics International*, vol. 45, no. 9, pp. 11826-11832, 2019.

[8] Z. Yin, S. Yan, J. Ye, Z. Zhu, J. Yuan, "Cutting performance of microwave-sintered sub-crystal Al2O3/SiC ceramic tool in dry cutting of hardened steel," *Ceramics International*, vol. 45, no. 13, pp. 16113-16120, 2019.

[9] C.S. Kumar, H. Majumder, A. Khan, S.K. Patel, "Applicability of DLC and WC/C low friction coatings on Al2O3/TiCN mixed ceramic cutting tools for dry machining of hardened 52100 steel," *Ceramics International*, 2020.

[10] A. Hadzley, T. Norfauzi, U. Umar, A. Afuza, M. Faiz, M. Naim, "Effect of sintering temperature on density, hardness and tool wear for alumina-zirconia cutting tool," *Journal of Mechanical Engineering and Sciences*, vol. 13, no. 1, pp. 4648-4660, 2019.

[11] D. Moghadam, E. Omrani, P. L. Menezes, P.K. Rohatgi, "Mechanical and tribological properties of self-lubricating metal matrix nanocomposites reinforced by carbon nanotubes (CNTs) and graphene–a review," *Composites Part B: Engineering*, vol. 77, pp. 402-420, 2015.

[12] D.S. Lim, D.H. You, H.J. Choi, S.H. Lim, H. Jang, "Effect of CNT distribution on tribological behavior of alumina–CNT composites," *Wear*, vol. 259, no. 1-6, pp. 539-544, 2005.

[13] V. Puchy, P. Hvizdos, J. Dusza, F. Kovac, F. Inam, and M. Reece, "Wear resistance of Al2O3–CNT ceramic nanocomposites at room and high temperatures," *Ceramics International*, vol. 39, no. 5, pp. 5821-5826, 2013.

[14] M. Hajiaboutalebi, M. Rajabi, and O. Khanali, "Physical and mechanical properties of SiC-CNTs nano-composites produced by a rapid microwave process," *Journal of Materials Science: Materials in Electronics*, vol. 28, no. 12, pp. 8986-8992, 2017.

[15] J. Sun, L. Gao, and W. Li, "Colloidal processing of carbon nanotube/alumina composites," *Chemistry of Materials*, vol. 14, no. 12, pp. 5169-5172, 2002.

[16] H. Porwal, M. Kasiarova, P. Tatarko, S. Grasso, J. Dusza, and M. Reece, "Scratch behaviour of graphene alumina nanocomposites," *Advances in Applied Ceramics*, vol. 114, no. sup1, pp. S34-S41, 2015.

[17] M. S. A. Shambharkar, M. A. W. Kawale, and M. C. J. Choudhari, "Analysis of Single Point Cutting Tool Using ANSYS," *International Journal on Recent and Innovation Trends in Computing and Communication*, vol. 4, no. 5, pp. 331-338, 2016.

[18] G. Pintaude, "Introduction of the Ratio of the Hardness to the Reduced Elastic Modulus for Abrasion," *Tribology-Fundamentals and Advancements: IntechOpen*, 2013.

[19] U. Holzwarth, and N. Gibson, "The Scherrer equation versus the'Debye-Scherrer equation'," *Nature Nanotechnology*, vol. 6, no. 9, pp. 534-534, 2011.

[20] N. Bakhsh, F. A. Khalid, and A. S. Hakeem, "Synthesis and characterization of pressureless sintered carbon nanotube reinforced alumina nanocomposites," *Materials Science and Engineering: A*, vol. 578, pp. 422-429, 2013.

[21] G.D. Zhan, J.D. Kuntz, J. Wan, and A.K. Mukherjee, "Single-wall carbon nanotubes as attractive toughening agents in alumina-based nanocomposites," *Nature materials*, vol. 2, no. 1, pp. 38-42, 2003.

[22] M. N. Rahaman, Ceramic processing and sintering: CRC press, 2017.

[23] A. Peigney, F.L. Garcia, C. Estournes, A. Weibel, and C. Laurent, "Toughening and hardening in double-walled carbon nanotube/nanostructured magnesia composites," *Carbon*, vol. 48, no. 7, pp. 1952-1960, 2010.

[24] P. Samal, S.S. Mohanty, M. Panigrahi, and S. Mohanty, "Finite element analysis of the dental crown: a case study of alumina-based incisor", p. 012003, IOP Conf. Series: *Materials science and Engineering* 410, 2018.